JACS
JOURNAL OF THE AMERICAN CHEMICAL SOCIETY

Article

pubs.acs.org/JACS

Multitriggered Shape-Memory Acrylamide–DNA Hydrogels

Chun-Hua Lu,[†] Weiwei Guo,[†] Yuwei Hu,[†] Xiu-Juan Qi,[†,‡] and Itamar Willner*[,†]

[†]The Institute of Chemistry, The Minerva Center for Biohybrid Complex Systems, The Hebrew University of Jerusalem, Jerusalem 91904, Israel

[‡]The Key Laboratory of Analysis and Detection Technology for Food Safety of the MOE, College of Chemistry, Fuzhou University, Fuzhou 350002, China

Supporting Information

ABSTRACT: Acrylamide–acrylamide nucleic acids are cross-linked by two cooperative functional motives to form shaped acrylamide–DNA hydrogels. One of the cross-linking motives responds to an external trigger, leading to the dissociation of one of the stimuli-responsive bridges, and to the transition of the stiff shaped hydrogels into soft shapeless states, where the residual bridging units, due to the chains entanglement, provide an intrinsic memory for the reshaping of the hydrogels. Subjecting the shapeless states to counter stimuli restores the dissociated bridges, and regenerates the original shape of the hydrogels. By the cyclic dissociation and reassembly of the stimuli-responsive bridges, the reversible switchable transitions of the hydrogels between stiff shaped hydrogel structures and soft shapeless states are demonstrated. Shaped hydrogels bridged by K^+-stabilized G-quadruplexes/duplex units, by i-motif/duplex units, or by two different duplex bridges are described. The cyclic transitions of the hydrogels between shaped and shapeless states are stimulated, in the presence of appropriate triggers and counter triggers (K^+ ion/crown ether; pH = 5.0/8.0; fuel/antifuel strands). The shape-memory hydrogels are integrated into shaped two-hydrogel or three-hydrogel hybrid structures. The cyclic programmed transitions of selective domains of the hybrid structures between shaped hydrogel and shapeless states are demonstrated. The possible applications of the shape-memory hydrogels for sensing, inscription of information, and controlled release of loads are discussed.

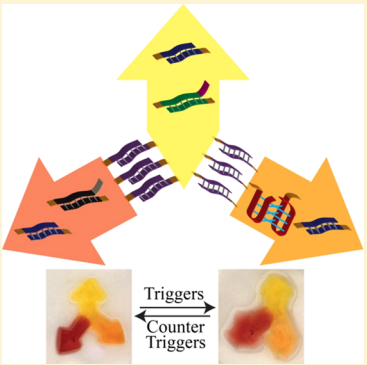

INTRODUCTION

Shape-memory polymers represent an interesting class of materials that might reveal new applications. The shape-memory polymers are processed into shaped structures that undergo, in the presence of appropriate stimuli, transitions into shapeless structures. The shapeless polymers are programmed to include an internal memory that restores the original shaped structures in the presence of appropriate counter stimuli.[1] Different applications of shape-memory polymers were suggested, including their function as actuators of micro-devices,[2] drug release systems,[3] and inscription of information.[4] For the successful design of shape-memory polymers, two basic features should be fulfilled: (i) The polymer should undergo a stimuli-responsive structural transition. (ii) The polymer should be programmed to include a chemical or physical memory code to recover under appropriate conditions to the original permanent polymer shape. The base sequence in nucleic acids (DNA) encodes for structural and functional information in the biopolymers.[5] Different external stimuli, such as pH,[6] metal ion/ligand,[7] or photonic signals,[8] were applied to reversibly reconfigure DNA structures, such as i-motif,[9] duplex nucleic acids,[10] or G-quadruplexes,[11] and these processes were used to assemble DNA switching devices and DNA machines.[12] DNA-based hydrogels attract recent research interest as a functional material.[13] Two different strategies were used to assemble DNA hydrogels. By one method, "all-DNA" hydrogels were constructed by the cross-linking of toehold-modified DNA branched subunits, e.g., Y-shaped units, by duplex DNA bridges, that result in cross-linked porous DNA networks in the form of hydrogels.[14] The second approach involves the modification of polymer chains, e.g., polyacrylamide with nucleic acid tethers. The cross-linking of the polymer chains by means of the nucleic acid tethers, e.g., via formation of nucleic acid duplexes, resulted in the cross-linking of the polymer chains and the formation of hydrogels.[15] With tailored stimuli-responsive DNA bridges, switchable DNA-based hydrogels undergoing one-cycle or multicycle hydrogel-to-solution phase transitions were assembled.[16] For example, by the pH-stimulated bridging of nucleic-acid-functionalized polymers by means of i-motif[16f] or triplex[17] DNA nanostructures, the formation and dissociation of hydrogels were demonstrated. Similarly, the bridging of nucleic acids by ion-assisted formation of duplex DNAs[16a] or K^+-ion-assisted formation of G-quadruplexes[16b] and the dissociation of the metal-ion-stabilized nanostructures by appropriate ligands or receptors,[16c] led to the assembly of stimuli-responsive hydrogels that undergo reversible hydrogel-to-solution phase transitions. Different applications of stimuli-responsive hydrogels were suggested, including controlled drug release,[18] sensors,[19] separating substrates,[20] and the triggered activation of enzyme cascades.[21] Recently, a DNA shape-memory hydrogel that undergoes gel-

Received: June 23, 2015
Published: November 18, 2015

DOI: 10.1021/jacs.5b06510
J. Am. Chem. Soc. 2015, 137, 15723–15731

to-quasisolid transition was reported.[22] Also, DNA/polyacrylamide hybrids were used to assemble shape-memory hydrogels.[23] In these systems, the acrylamide chains were modified with two controllable DNA functions. One of the DNA functions associated with the tethers included domains with base pair complementarity that led to the cross-linking of the chains. The other nucleic acid tethers associated with the polymer chains included C-rich tethers that cross-linked the chains at pH = 5.0 by i-motif units. The cooperative cross-linking of the chains by the duplex bridging units and the i-motif structure resulted in the formation of a shaped hydrogel in a mold, and these cross-linking motives provided the interactions for retaining the permanent shape of the hydrogel, upon its exclusion from the mold. Neutralization of the shaped hydrogel, pH = 8.0, separated the i-motif bridges and dissociated the hydrogel to a quasiliquid phase. The remaining duplex bridges are insufficient to provide an energetically stabilized hydrogel, but the entangled cross-linked chains provide, in the resulting shapeless state, a temporary memory to reassemble the original permanent shape upon the acidification of the system, and the reformation of the i-motif bridges. Nonetheless, this pH-stimulated shape-memory hydrogel stands as a single example for this paradigm, and the broadening of the concept to other shape-memory triggers is a challenge. In the present study, we demonstrate that other reversible switchable cross-linking units, e.g., K^+-stabilized G-quadruplex/crown ether or fuel/antifuel strands, coupled to permanent duplex nucleic acid cross-linking units, and acting as internal "shape memory", lead to functional shape-memory hydrogels. Besides enriching the "tool-box" of triggers that yield switchable shape-memory polymers, the novelty of the study rests on the fact that we demonstrate the ability to combine different stimuli-responsive shape-memory hydrogels into an integrated hybrid structure revealing programmable shape-memory properties. We demonstrate that the different domains, comprising the hybrid structure, can be individually or simultaneously addressed by appropriate triggers to yield dictated-reversible shape-to-shapeless transitions of the composite. It should be noted that switchable shape-memory hydrogels, undergoing reversible shaped-hydrogel/shapeless-matrix transitions between shaped and shapeless states, introduce enhanced complexities and functionalities to switchable DNA hydrogel materials. New applications, such as inscription, sensing, and, particularly, dictated growth of cells on shape-memory hydrogels, may be envisaged.

In the present study, we introduce two new hydrogel composites exhibiting shape-memory properties. In one system, the permanent shape of the hydrogel is stabilized by the cooperative bridging of the DNA–acrylamide hydrogel by K^+-stabilized G-quadruplex and duplex DNA cross-linking units. The 18-crown-6 ether (CE)-stimulated separation of the G-quadruplexes via the elimination of K^+ results in the separation of the hydrogel into a soft and shapeless state that includes the entangled duplex chains as a memory to re-form the shaped structure. In the second system, the permanent shape of the hydrogel is retained by the functionalization of the acrylamide chains with two different nucleic acids that cooperatively stabilize the formation of the hydrogel by two kinds of duplex DNA bridges. The separation of one of the duplexes via a strand displacement process leads to a shapeless state that retains the second duplex as an internal shape memory. The reformation of the two bridging duplexes units regenerates the permanent shape of the hydrogel being stabilized by the two kinds of duplexes. We further demonstrate the integration of hybrid structures that include two or three shape-memory hydrogel materials that can be separately or, simultaneously, triggered across shapeless and shaped domains, using two or three triggering stimuli.

RESULTS AND DISCUSSION

Figure 1A depicts the operation of the G-quadruplex/duplex DNA permanent shape hydrogel. The acrylamide copolymer

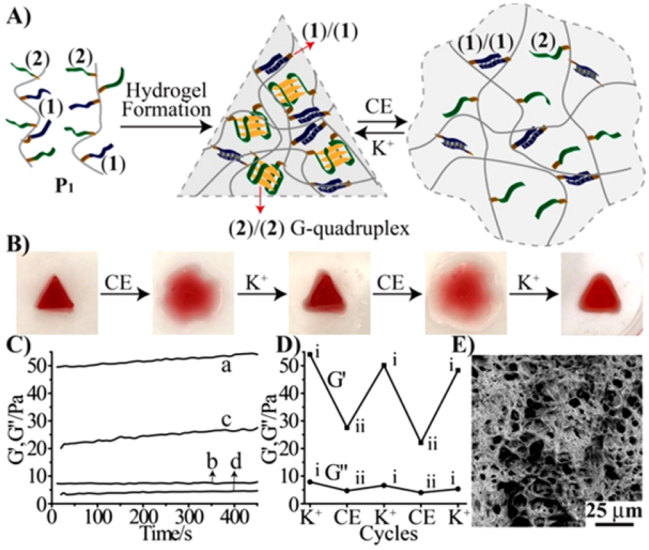

Figure 1. (A) Schematic synthesis and function of the duplex/G-quadruplex-cross-linked shape-memory hydrogel. Treatment of the hydrogel with CE results in the dissociation of the stiff and shaped hydrogel to the soft and shapeless state, exhibiting the shape-memory duplex element. The subsequent treatment of the shapeless state with K^+ ions restores the shaped duplex/G-quadruplex structure. (B) Images corresponding to the switchable transitions of the system between the hydrogel triangle shape and the shapeless quasiliquid. (C) Rheometric characterization of the hydrogel/quasiliquid state. (a) G' of the hydrogel; (b) G'' of the hydrogel; (c and d) G' and G'' of the quasiliquid state. (D) Switchable transitions of the G' and G'' values corresponding to the hydrogel (i) and quasiliquid (ii) states where the states (i) are generated in the presence of added K^+ and states (ii) are generated in the presence of CE. (E) SEM image of the freeze-dried hydrogel coated with a thin layer of Au/Pd.

chains P_1 were prepared by polymerization of the acrylamide monomer and the (**1**)-acrydite and (**2**)-acrydite monomers at a ratio 1:6. The loading of the DNA on the acrylamide copolymer corresponded to acrylamide nucleic acid tethers: acrylamide = 21:1 (for the determination of the loading see Figure S1, Supporting Information). The strand (**1**) includes a self-complementary sequence, while the strand (**2**) consists of a sequence corresponding to half of a G-quadruplex. The (heated) liquid aqueous mixture of P_1 was introduced into a triangular mold, and after cooling to room temperature, a solution of K^+ ions was added to the viscous composite in the mold. This resulted in the formation of the hydrogel stabilized by the cooperative cross-linking bridges consisting of the duplexes (**1**)/(**1**) and the K^+-stabilized G-quadruplexes (**2**)/(**2**). The resulting triangle-shaped hydrogel was extracted from the mold. Treatment of the shaped hydrogel with 18-crown-6 ether, CE, eliminated the K^+ ions from the G-quadruplex bridges. The dissociation of the G-quadruplex units separated the hydrogel into a shapeless structure. The duplex bridging

DOI: 10.1021/jacs.5b06510
J. Am. Chem. Soc. 2015, 137, 15723–15731

units are retained in the shapeless polymer mixture, but their density is insufficient to stabilize a cross-linked shaped hydrogel structure. The residual duplex bridges entangled in the polymer network provide, however, an "internal memory", and upon the readdition of K^+ ions, the original triangle-shaped hydrogel, cooperatively stabilized by (**1**)/(**1**) bridges and G-quadruplexes, (**2**)/(**2**) is formed. The cyclic switching of the triangle-shaped hydrogel into a shapeless droplet and back to the triangle shape is shown in Figure 1B. The system could be switched for at least three cycles between shaped and shapeless states. Rheometric characterization of the cooperatively stabilized (**1**)/(**1**):(**2**)/(**2**), Figure 1C, curves a and b (G' = 54 Pa, G'' = 7.8 Pa), and of the shapeless mixture, Figure 1C, curves c and d (G' = 27 Pa, G'' = 4.6 Pa), confirms that the (**1**)/(**1**) G-quadruplex, (**2**)/(**2**), matrix exists indeed, as a hydrogel while the CE-treated hydrogel exists as a soft, shapeless mixture. Figure 1D shows the cyclic changes in the storage modulus of the system, G', upon treatment of the copolymer, P_1, mixture with K^+ ions and CE between shaped hydrogel and shapeless states. The existence of the (**1**)/(**1**):(**2**)/(**2**)-cross-linked system as a hydrogel and its transition to the (**1**)/(**1**) cross-linked soft and shapeless state are supported by the fact that the G'/G'' for the hydrogel state exhibits the value 7.5, while for the shapeless state G'/G'' corresponds to 4.5. The relatively high G'/G'' value for the shapeless state is attributed to the relatively high loading of the duplexes in the system (required to retain the shape of the hydrogel state) that leads to a relatively stiff shapeless state. Figure 1E depicts the SEM image of the (**1**)/(**1**)/G-quadruplex, (**2**)/(**2**), cross-linked hydrogel. (For the comparison of the SEM images of the hydrogel and shapeless states, see Figure S2, Supporting Information.) The dissolution of the shaped hydrogel in the presence of CE and the recovery of the shaped hydrogel upon addition of K^+ ions occurred on a time-scale of 2 h. It should be noted that the fully triangle-shaped G-quadruplex-cross-linked hydrogel (that lacks the (**1**)/(**1**) bridges) was dissolved upon the addition of CE into a liquid shapeless structure. Upon the addition of K^+ ions, the droplet was transformed into a shapeless hydrogel, thus supporting our explanation that the duplex bridges (**1**)/(**1**) present in the quasiliquid system shown in Figure 1 provide an internal memory for the reshaping of the hydrogel. (For the results of this control experiments see Figure S3, Supporting Information.)

The construction and functions of the hybrid shape-memory hydrogel responding to G-quadruplex and pH triggers are presented in Figure 2. The system, Figure 2A, is composed of the domain A, where the acrylamide chains are cross-linked, at pH = 5.0, by the duplex (**1**)/(**1**) and the i-motif subunits (**3**)/(**3**). At pH = 8.0, the i-motif bridges are separated to yield a quasiliquid phase that includes the duplexes (**1**)/(**1**) as memory element. (This pH-sensitive shape-memory hydrogel was recently characterized by our group,[23] Figures S4–S6, Supporting Information.) The second domain, B, is the (**1**)/(**1**):(**2**)/(**2**) duplex/G-quadruplex-cross-linked hydrogel. Figure 2B depicts the method to construct the hybrid shaped structure of the two domains. Domain A was generated in a mold (arrow shape) separated by a stopper from a second mold arrow-shaped reservoir in the mold. Subsequent to the formation of the domain A, the stopper was removed, and the hot solution of the liquified components of domain B was added to the empty mold reservoir; the mixture was allowed to cool down to form the (**1**)/(**1**):(**2**)/(**2**)-cross-linked hydrogel. The contact edge between domains B and A includes, however,

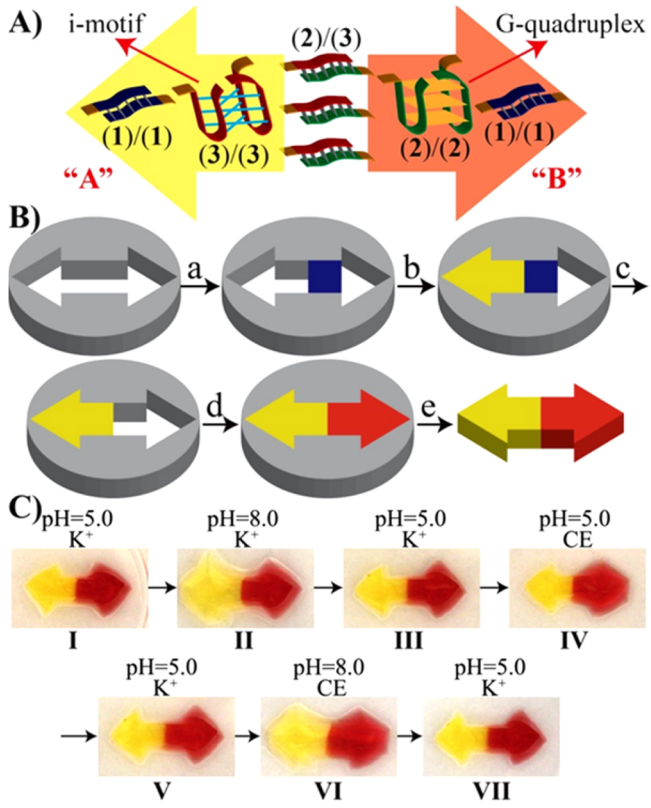

Figure 2. (A) Schematic structure of a stimuli-responsive hybrid hydrogel exhibiting two shape-memory domains, A and B; a pH-sensitive i-motif/random coil domain (yellow) and a K^+-stabilized G-quadruplex/CE responsive domain (red). (B) Schematic assembly of the shaped hybrid hydrogel that includes two different shape-memory elements: (a) Blocking the two-arrowhead mold with a blocker unit (blue); (b) assembly of the duplex/i-motif arrowhead domain, A, (yellow); (c) removal of the blocker unit; (d) growing the duplex/G-quadruplex-cross-linked hydrogel in the vacant reservoir; (e) removal of the hybrid hydrogel from the mold. (C) Images corresponding to the stimuli-triggered transitions of the two-shape-memory hydrogel between stiff and shaped hydrogel structures and soft shapeless states: (I) The two-arrowhead-shaped hydrogel consisting of i-motif/duplex:G-quadruplex/duplex-cross-linked matrices. (II) After treatment of the hybrid hydrogel at pH = 8.0 and dissociation of the yellow arrowhead, domain A. (III) After treatment of the resulting system at pH = 5.0 and recovery of the shaped two arrowhead structure. (IV) Treatment of the system with CE and dissociation of the G-quadruplex bridges in domain B and the transition of domain B into a quasiliquid state. (V) Treatment of the resulting system with K^+ ions and the regeneration of the two arrowhead structures. (VI) Treatment of the system at pH = 8.0 and in the presence of CE. Dissociation of the i-motif and G-quadruplex bridges leads to the transition of domains A and B into quasiliquid states. (VII) Treatment of the system at pH = 5.0 and in the presence of K^+ ions restores the shaped two arrowhead structure.

complementary G-rich and C-rich domains of (**2**)/(**3**), resulting in their hybridization and the formation of an interconnected hybrid of domains A and B. Domains A and B were labeled with SYBR Gold and Gel Red to yield yellow- and red-labeled arrow-shaped structures, respectively. The resulting structure was removed from the mold, resulting in an intact stable hydrogel structure of the two domains, Figure 2C. Physical agitation of the interconnected domains did not lead to the separation of the two hydrogels, implying that the hybridization of strands (**2**)/(**3**) is sufficiently strong to retain

DOI: 10.1021/jacs.5b06510
J. Am. Chem. Soc. 2015, 137, 15723–15731

the two stable domain hydrogel structures. It should be noted that preparation of the individual hydrogels A and B did not, even after prolonged shaking, form the interconnected hybrid of domains A and B (Figure S7, Supporting Information). We assume that the warm mixture of domain B melts the contact edge of domain A, in the course of preparation, thus allowing increased hybridization between strands (**2**) and (**3**) at the boundary domain linking the two domains. Figure 2C depicts the shape-memory control of the hybrid two-domain structure using pH and K^+ ions/CE as triggers. The primary hybrid structure consists of two shaped arrows ((**1**)/(**1**):(**3**)/(**3**)-yellow) and (**1**)/(**1**):(**2**)/(**2**)/-red), that are stabilized at pH = 5.0 and in the presence of K^+ ions, respectively. Subjecting the system to pH = 8.0 distorts the yellow arrow into a quasiliquid shapeless structure without affecting the shape of domain B. These results are consistent with the separation of the i-motif bridging units in domain A and its transition to a quasiliquid state. Reacidification of the system to pH = 5.0 restores the arrow shape of domain A, implying that the quasiliquid state included the shape-memory element provided by the entangled duplex bridges (**1**)/(**1**). Subsequent treatment of the two-arrow hybrid with CE transformed domain B (red arrow) into a shapeless state. Further addition of K^+ ions regenerated the two arrow-shaped hybrid structures of domains A and B. These results are consistent with the selective pH- or CE-stimulated dissociation of domains A or B into shapeless states that retain internal "memories" to reshape the respective hydrogels. Finally, the hybrid two-arrow-shaped hydrogel was treated, simultaneously, with the two triggers pH = 8.0 and CE. The reverse treatment of the system with K^+ ions at pH = 5.0 restores the two-arrow-shaped structure, implying that the shape-memory is retained in the two original hydrogels. The pH-stimulated dissolution of the (**1**)/(**1**):(**3**)/(**3**)-cross-linked shaped hydrogel domain and the recovery of the shaped structure occurred on a time-scale of 30 min. The dissolution of the (**2**)/(**2**):(**1**)/(**1**)-cross-linked hydrogel domain and the recovery of the shaped structure occurred on a time-scale of 2 h.

A further method to construct a shape-memory hydrogel has involved the use of the strand displacement principle, Figure 3A. The system involves the use of an acrylamide/acrylamide nucleic acid copolymer chain, P_2. The chain P_2 was functionalized with the nucleic acid (**1**), exhibiting self-complementarity, and with the nucleic acids A_1 (**4**) and A_2 (**5**), where (**4**) and (**5**) exhibit partial complementarities. This chain was synthesized by the polymerization of acrylamide and acrydite-(**1**), acrydite-(**4**), and acrydite-(**5**) monomers at a ratio of 8:9:9. The loading of acrylamide:acrylamide nucleic acids tethers corresponded to 51:1 (Figure S8, Supporting Information). The two kinds of duplexes, (**1**)/(**1**) and (**4**)/(**5**) (A_1/A_2), cross-linked the chains, resulting in the cooperative stabilization of the hydrogel. The nucleic acid A_2 (**5**) includes a single-strand toehold, and thus, treatment of the hydrogel with strand A_3 (**6**), exhibiting complementarity to A_2 (**5**), results in the formation of the energetically stabilized duplex A_2/A_3 (**5**)/(**6**). This leads to the formation of a shapeless state, where the duplexes (**1**)/(**1**) provide the shape-memory entangled cross-linking network. (The formation of the duplex A_2/A_3 is energetically favored, and this provides the driving force for the strand displacement process.) The strand A_3 (**6**) includes, also, a single-strand toehold, and in the presence of the auxiliary strand A_4 (**7**), the formation of the energetically stabilized duplex A_3/A_4 (**6**)/(**7**) is favored. This results in the separation of the

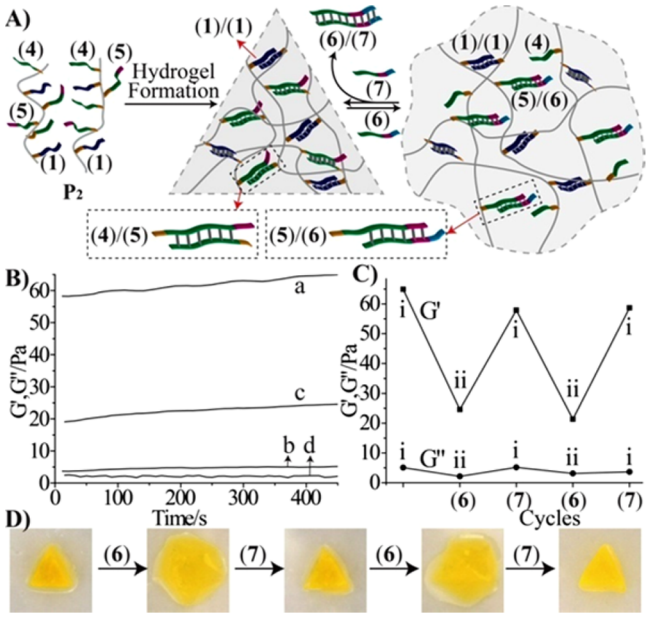

Figure 3. (A) Synthesis of the triangle-shaped hydrogel-cross-linked by two different duplexes (**1**)/(**1**) and (**4**)/(**5**) and the switchable transitions of the hydrogel between the shaped gel structure and shapeless state, and back, using the strand displacement mechanism. The (**1**)/(**1**) duplexes in the quasiliquid phase provide the stored memory for reshaping the hydrogel. (B) Rheometric characterization of the hydrogel and quasiliquid states of the system: (a) time-dependent G' of the hydrogel; (b) G'' of the hydrogel; (c) time-dependent G' of the quasiliquid; (d) G'' of the quasiliquid (G', storage modulus; G'', loss modulus). (C) Switchable transitions between the hydrogel and quasiliquid states stimulated by the strand displacement mechanism: (i) Hydrogel system consists of the (**1**)/(**1**) and (**4**)/(**5**) cross-linked matrix. (ii) Quasiliquid system consists of the (**1**)/(**1**) cross-linked matrix and (**5**)/(**6**) non-cross-linked duplexes. (D) Images corresponding to the cyclic transitions between the shaped triangle structure and the shapeless soft state upon treatment of the systems with strands (**6**) and (**7**), respectively.

duplex A_3/A_4 and the reformation of the hydrogel. By the cyclic addition of A_3 and A_4, the reversible transitions of the system between the quasiliquid and hydrogel states proceed. The duplex (**1**)/(**1**) in the shapeless state provides the memory for the reshaping of the hydrogel. Figure 3B shows the time-dependent features of the storage modules, G', and of the loss modules, G'', corresponding to the hydrogel (curves a and b, respectively) and of the quasiliquid state (curves c and d, respectively). Figure 3C depicts the rheology experiments demonstrating the switchable cyclic G' and G'' values upon transforming the hydrogel to the quasiliquid state. The existence of the (**1**)/(**1**):(**4**)/(**5**)-cross-linked system as a hydrogel and the dissolution of the hydrogel into the (**1**)/(**1**)-cross-linked quasiliquid state are supported by the fact that $G'/G'' \approx 12.9$ in the hydrogel state and $G'/G'' \approx 8.1$ in the quasiliquid state. For the SEM images of the hydrogel see Figure S9, Supporting Information. Figure 3D shows the cyclic transitions of a shaped hydrogel structure to the quasiliquid state and back. Further support for the triggered dissolution of the (**1**)/(**1**):(**4**)/(**5**) bridged hydrogel to the quasiliquid phase upon the strand-displacement of (**6**) by means of (**7**) was obtained by following the release of a dye (Oregon Green Dextran, MW = 70 KD) from the hydrogel matrix, Figure S10, Supporting Information. While the dye leaks out slowly from the hydrogel matrix, the dissolution of the hydrogel in the

DOI: 10.1021/jacs.5b06510
J. Am. Chem. Soc. 2015, 137, 15723−15731

presence of (**6**) leads to the fast release of the incorporated dye. It should be noted that the dissolution of the (**1**)/(**1**):(**4**)/(**5**)-cross-linked shaped hydrogel, in the presence of the "fuel" strand (**6**), and the recovery of the shapeless matrix to the shaped structure, upon addition of the "anti-fuel" (**7**), occurred on a time-scale of 4 h.

Figure 4A depicts schematically the integration of two systems of acrylamide/acrylamide nucleic acid copolymer chains, P_3 and P_4, operating by the strand displacement principle, and used to construct a hybrid hydrogel system that includes two shape-memory domains composed of domains A and B. The domain A, composed of P_3, included cross-linking units (**1**)/(**1**) and A_1/A_2 (**4**)/(**5**), and an additional tether L_1 (**8**). Similarly, domain B, composed of P_4, included tether L_2 (**9**) and the self-complementary bridges (**1**)/(**1**) and strands B_1 (**10**) and B_2 (**11**). The nucleic acid tethers L_1 and L_2 exhibit complementarity, thus allowing the binding of the two domains one to another to form the hybrid hydrogel system. The cross-linking of the polymer chains P_4 by the duplexes (**1**)/(**1**) and B_1/B_2 (**10**)/(**11**) yields the cooperatively stabilized domain B. The treatment of domain B with strand B_3 (**12**) results in the separation of the duplex $(B_1)/(B_2)$, (**10**)/(**11**), and the formation of $(B_2)/(B_3)$, (**11**)/(**12**), leading to the transition of the domain B to a soft and shapeless state cross-linked by the bridges (**1**)/(**1**) that provide the memory for the reformation of the shaped hydrogel. Subjecting the shapeless system to strand B_4 (**13**) leads to the displacement of B_3 from B_2/B_3 that produces the energetically stabilized "waste" duplex B_3/B_4, (**12**)/(**13**). This process restores the shaped (**1**)/(**1**):(**10**)/(**11**), cooperatively stabilized domain B. The rheometry experiments characterizing domain B, and the switchable shape-memory transitions of domain B between the hydrogel and quasiliquid states are presented in Figure S11, Supporting Information. The two domains A and B were integrated into a composite system by the hybridization of the tethers L_1 and L_2, (**8**) and (**9**), in the mold (for the method generating the nonseparable hybrid of domains A and B, *vide supra*), Figure 4B. The structure composed of the two domains was removed from the mold, and then subjected to the triggered switchable transitions between the shape-memory hydrogel and the quasiliquid states in the presence of A_3 or A_4, (**6**) or (**7**), and/or B_3 or B_4, (**12**) or (**13**), respectively, Figure 4C. Treatment of the composite, two-arrowheads, hydrogel, image I, with strand A_3 (**6**), transformed domain A (yellow) into a shapeless form, while domain B (red) retained its structure, image II. Subjecting the resulting system to A_4 (**7**) regenerated the original yellow shaped domain A, image III. Further treatment of the two-arrowhead hybrid with strand B_3 (**12**) resulted in the separation of domain B, and the formation of the soft, red, shapeless domain, image IV. The subsequent treatment of the system with strand B_4 (**13**) restored the shaped two-arrowheads composite hydrogel, image V. Finally, the system was subjected to both strands, A_3 (**6**) and B_3 (**12**), and this led to the formation of two shapeless red/yellow domains, image VI. The treatment of the resulting structure with strands A_4 (**7**) and B_4 (**13**) regenerated the shaped composite structure of the two domains, image VII.

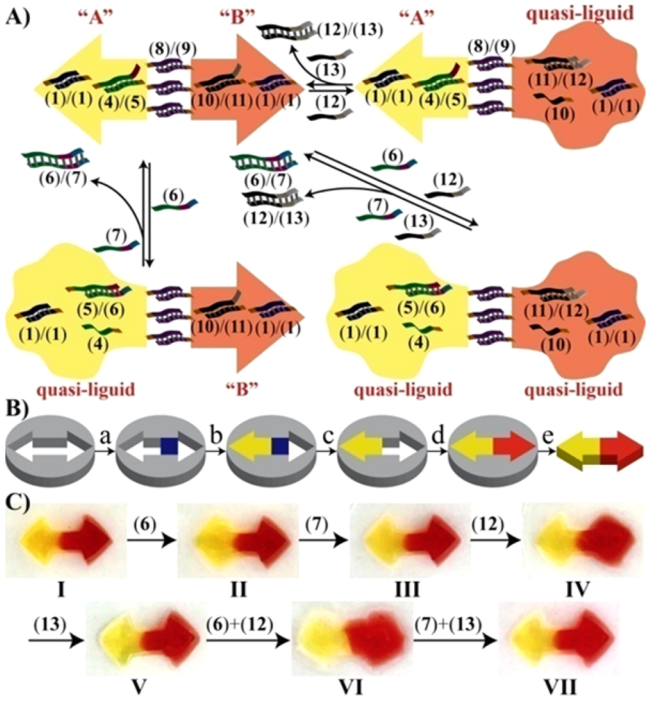

Figure 4. (A) Cyclic switchable transitions of the hybrid two-arrowhead-shaped hydrogel composed of two domains A and B, each exhibiting a shape-memory element. The reversible transitions across the states are stimulated by the strand displacement principle. (B) Schematic presentation of the preparation of the hybrid hydrogel consisting of the arrowhead domain A and B: (a) blocking the mold with the stopper (blue); (b) growing the hydrogel of domain A (yellow) in the stoppered mold; (c) removal of the stopper from the mold and (d) growing to hydrogel of domain B in the vacant reservoir; (e) removal of the hybrid two arrowhead composite from the mold. (C) Images corresponding to the reversible transitions of the shape-memory hybrid hydrogel across the different states: (I) Arrowhead hybrid structures of domains A and B. (II) Transformation of domain A into a soft and shapeless state that included the duplex (**1**)/(**1**) as memory elements via strand displacement of the duplex (**4**)/(**5**) with (**6**). (III) Regeneration of the two-arrowhead structure by the addition of strand (**7**) and the displacement of strand (**6**) via formation of the "waste" (**6**)/(**7**) duplex, and the reformation of duplex (**4**)/(**5**). (IV) Transformation of domain B in the two-arrowhead structure into the soft and shapeless phase that includes the (**1**)/(**1**) duplex as memory elements via the (**12**)-stimulated strand displacement of duplex (**10**)/(**11**). (V) Regeneration of the hybrid two-arrowhead structure by (**13**)-triggered displacement of (**12**) and the formation of the waste (**12**)/(**13**) duplex, and the concomitant formation of the (**10**)/(**11**) duplex. (VI) The transition of domains A and B into shapeless states using the strand displacement of (**4**)/(**5**) and (**10**)/(**11**) by (**6**) and (**12**), respectively. (VII) Regeneration of the two-arrowhead structure by the displacement of (**6**) and (**12**) from the shapeless domains A and B by (**7**) and (**13**) to form the (**6**)/(**7**) and (**12**)/(**13**) waste duplexes, and the concomitant formation of the duplexes (**4**)/(**5**) and (**10**)/(**11**).

To this end, a hybrid composite of three shaped domains, A, B, and C, was subjected to three shape-memory triggers as outlined in Figure 5A. The system was constructed of the two domains A and B triggered by the strands A_3 or A_4, (**6**) or (**7**), and B_3 or B_4, (**12**) or (**13**), respectively, and of the pH-responsive domain C that includes the i-motif-triggered transitions of the bridges (**3**)/(**3**), cf., Figure 2 and accompanying discussion. As shown in Figure 5B, in the first step, domain A that was cross-linked by the bridges (**1**)/(**1**) and A_1/A_2 (**4**)/(**5**) was prepared in the mold. This domain (yellow) was functionalized with the tethers L_1 (**8**), for hybridization with the other domains. The shape of the domain A in the mold included an arrowhead, and its stem contained two edges for the stepwise binding of domains B and C. Upon

DOI: 10.1021/jacs.5b06510
J. Am. Chem. Soc. 2015, 137, 15723−15731

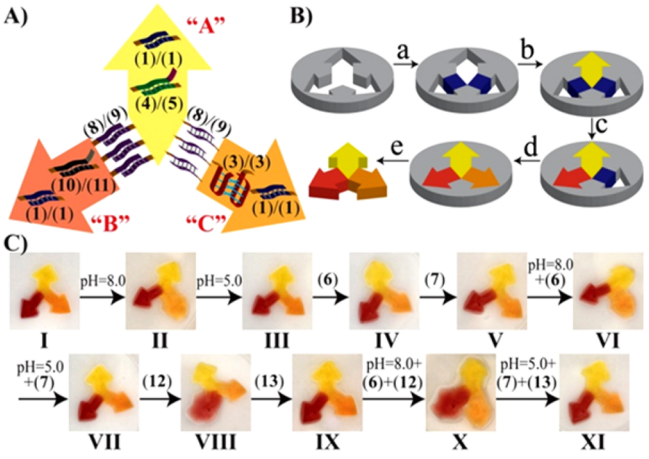

Figure 5. (A) Schematic structures of a stimuli-responsive hybrid, three-arrowhead structure consisting of domains A, B, and C, and exhibiting three shape-memories. The structure undergoes hydrogel-to-quasiliquid transitions by strand displacement triggers (domains A and B) and by three-arrowhead pH (domain C). (B) Schematic preparation of the hybrid three-arrowhead structure exhibiting three shape-memory elements. (C) Images correspond to the reversible hydrogel/quasiliquid transitions in the hybrid three-arrowhead structure. (I) The as-prepared three-arrowhead structures. (II) The pH-stimulated transition of domain C into the quasiliquid state. (III) The pH-stimulated regeneration of the three-arrowhead structures. (IV) The transition of domain A into the quasiliquid state by the (**6**)-induced strand displacement process. (V) Regeneration of the three-arrowhead structure by the strand displacement of (**6**) from domain A, and the formation of the (**6**)/(7) "waste". (VI) Transition of domains A and C into quasiliquid states by subjecting the structure to the (**6**)-stimulated strand displacement and pH = 8.0, respectively. (VII) Regeneration of the three-arrowhead structure by the (7)-stimulated strand displacement of (**6**) and formation of the (**6**)/(7) duplex "waste" and subjecting the system to pH = 5.0. (VIII) Transition of domain B into a quasiliquid phase using the (**12**)-stimulated displacement of (**10**)/(**11**). (IX) Regeneration of the hybrid three-arrowhead structure by the displacement of (**12**) with (**13**) and the formation of the (**12**)/(**13**) duplex as "waste". (X) The transition of domains A, B, and C into quasiliquid states using the strands (**6**) and (**12**) as strand displacers, respectively, and pH = 8.0 for converting domain C into the quasiliquid state. (XI) The regeneration of the three-arrowhead structure by treatment of the system with strands (7) and (**13**) to displace (**6**) and (**12**), respectively, and subjecting the system to pH = 5.0.

forming domain A, the two edges were separated by stoppers from the reservoirs for the preparation of domains B and C. The subsequent addition of the heated solution of chain P_3 modified with (**1**), L_2 (**9**), B_1 (**10**), and B_2 (**11**) to one of the reservoirs, while excluding the stopper, resulted in the formation of the domain B (red) cross-linked (**1**)/(**1**) and (**10**)/(**11**), and bridged to domain A by the duplex L_1/L_2, (**8**)/(**9**). In the final step, the heated mixture of the acrylamide chains modified with (**1**), (**3**), and L_2 (**9**), at pH = 5.0, was added to the third reservoir, while excluding the appropriate stopper. The resulting domain was cross-linked by the (**1**)/(**1**), (**3**)/(**3**) (i-motif) bridges and was linked to domain A via the duplex L_1/L_2, (**8**)/(**9**). The resulting three-arrowhead structure composed of domain A (yellow), domain B (red), and domain C (orange) was removed from the mold. Figure 5C depicts the sequence of triggered shape-memory transitions of the three-domain hydrogel structure. The as-prepared structure, image I, was subjected to pH = 8.0 that dissociated domain C (orange) and transformed it to the soft and shapeless domain, image II. The subsequent treatment of the system at pH = 5.0 recovered the original three-arrowhead structure, image III. Subjecting the system to strand A_3 (**6**) dissociated the domain A (yellow), resulting in the shapeless domain, image IV. The subsequent treatment of the system with A_4 (7) regenerated the shaped three-domain hydrogel system, image V. The additional treatment of the shaped structure with strand A_3 (**6**) and the conditions of the system at pH = 8.0 resulted in the dissociation of domains A and C into shapeless domains, image VI, and the subsequent treatment of the system with A_4 (7) at pH = 5.0 recovered the original shaped structure, image VII. Similarly, treatment of the system with strand B_3 (**12**) led to the dissociation of domain B into shapeless domains, image VIII, and the subsequent addition of the strands B_4 (**13**) to the system regenerated the shaped structure of the hydrogel, image IX. Finally, the treatment of the shaped three-arrowhead structure with A_3 (**6**), B_3 (**12**), at pH = 8.0, dissociated all domains into shapeless domains, image X. Subjecting the system to strands A_4 (7), B_4 (**13**), at pH = 5.0, restored the shapes of all three-arrowheads, image XI. It should be noted that the order of applying the triggering inputs can be altered. We were able to switch two times the complete cycle of shape-memory states with no noticeable effect on the three arrowhead composite structure. It should be noted that the entire two-arrowhead or three-arrowhead hybrid structures shown in Figure 4 or 5 were subjected to the respective triggers, and only the stimuli-responsive domains of the structures responded to these triggers. It should be noted that the triggered dissolution of the hybrid shaped structures (two-arrowheads and three-arrowheads) in the presence of the appropriate stimuli, and the recovery of the respective shapes, occurred on the time-scales that were described for the individual domains.

■ CONCLUSIONS

The present study extended the concept of DNA-based shape-memory hydrogels. Until now only the cooperative cross-linking of hydrogels by duplex DNA and i-motif bridging units has been demonstrated. The present study has introduced new motives to generate shape-memory DNA-based hydrogels. These included the formation of shaped structures of the hydrogel by the cooperative cross-linking of the polymer chains by duplex nucleic acid bridges and K^+-ion-stabilized G-quadruplexes, and the cooperative cross-linking of the hydrogels by two different programmed nucleic acid duplexes. The separation of the G-quadruplexes by means of 18-crown-6 ether, or the separation of one of the duplex bridges by means of a strand displacement mechanism, led to the separation of the shaped hydrogels and to the formation of shapeless systems. The residual duplex nucleic acids in the shapeless systems provided the memory for the regeneration of the original structures of the hydrogels. The reshaping of the hydrogel structures was achieved by the reformation of the cooperative cross-linking interactions that stabilize the hydrogels, e.g., K^+ ions that stabilize the G-quadruplex bridging units or nucleic acid strands that remove the displacer strands that dissociated the original hydrogels. For all systems, cyclic and switchable transitions between the shaped hydrogel and the quasiliquid systems were demonstrated. The common principle for the design of the shape-memory hydrogels includes the design of a delicate balance between two cross-linking motives of the hydrogel chains that act cooperatively in stabilizing the hydrogel structures. The switchable removal of one of the

DOI: 10.1021/jacs.5b06510
J. Am. Chem. Soc. 2015, 137, 15723−15731

cross-linking motives dissociates the hydrogel into a soft and shapeless system that includes the second cross-linking element as internal memory for reshaping the original hydrogel structure. One may suggest other switchable cross-linking elements, such as pH-sensitive triplex nucleic acid structures, and the stabilization of duplex nucleic acid cross-linking structures by metal ions or photoisomerizable intercalators as triggers for the assembly of shape-memory hydrogels.

DNA-based shape-memory biopolymers represent a new class of materials. Two different approaches were reported to assemble the shape-memory DNA-based hydrogels. One approach has involved the enzymatic synthesis of nested DNA biopolymers undergoing shape-memory transitions between solid and shaped swollen hydrogels.[22] The second approach has involved the use of cooperative i-motif and duplex nucleic acids cross-linking units for the pH-triggered transition of a shaped hydrogel to shapeless quasiliquid that includes the duplex nucleic acid cross-linker units as "memory" elements.[23] The novelty of the present study is reflected by the introduction of a rich "tool-box" of triggers that yield functional shape-memory hydrogels. The paradigm of synthesizing "shape-memory" hydrogels by two cooperative cross-linking units, where one cross-linker acts as stimuli-responsive unit and the other as "memory" element to reshape the hydrogel, was generalized. Most importantly, we demonstrated the integration of different shape-memory hydrogels into hybrid structures that reveal programmable shape-memory properties. In the presence of appropriate triggers, the individual or simultaneous addressing of domains of the hybrid structure that dictated shape-to-shapeless transitions was demonstrated.

The stimuli-triggered transitions of the shaped hydrogels to the soft, shapeless, matrices suggest that loads incorporated in the hydrogels may be released upon transforming the shaped hydrogels to the soft matrices. Specifically, the design of a hybrid structure composed of two different shape-memory matrices, loaded with two different loads, may lead to the stimuli-dictated release of the loads, in the presence of appropriate triggers. Toward this goal, the hybrid two-arrowhead hydrogel shown in Figure 4A was implemented for the stimuli-controlled programmed release of two different fluorescent payloads associated with the domains "A" and "B" of the hybrid hydrogel. The fluorescent Oregon Green modified dextran (MW = 70 kDa, λem = 520 nm) was incorporated into domain "A" of the hybrid hydrogel, and the fluorescent tetramethylrhodamine-modified dextran (MW = 70 kDa, λ_{em} = 580 nm) was immobilized in domain "B" of the hybrid hydrogel. Figure 6 depicts the programmed stimuli-triggered release of the fluorescent loads from the hybrid structure. Treatment of the hybrid structure with the strand (**6**) results in the dissociation of domain "A" of the hybrid structure, while the structure of domain "B" is unaffected. This leads to the selective release of the Oregon Green dextran, Figure 6, panel I. Treatment of the hybrid structure with strand (**12**) leads to the selective dissociation of domain B of the structure and to the selective release of the tetramethylrhodamine-modified dextran, Figure 6, panel II. Treatment of the two-arrowhead hybrid hydrogel structure with the strands (**6**) and (**12**) dissolves the two domains "A" and "B", resulting in the release of the two fluorescent payloads, Oregon Green dextran and tetramethylrhodamine-modified dextran, Figure 6, panel III. In addition to the programmed release of payloads from the hybrid hydrogel composite, one might realize that the stimuli-controlled stiffness of the hybrid structure might control the growth of cells in dictated directions.

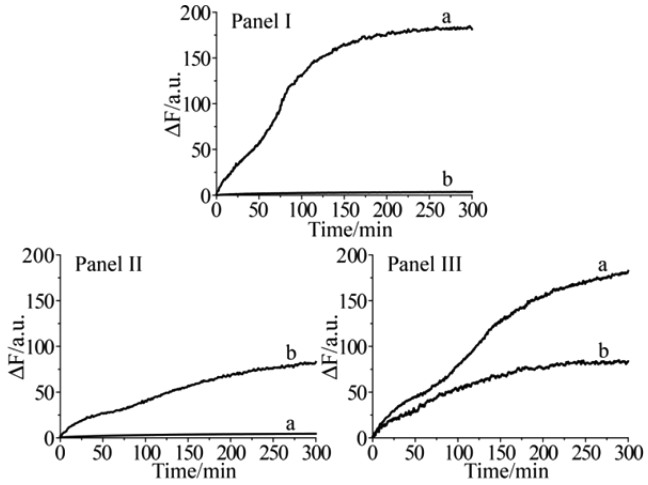

Figure 6. Time-dependent triggered release of the fluorescent payloads from the hybrid two-arrowhead hydrogel structure upon the following treatments: panel I, treatment of the structure with strand (**6**), where (a) corresponds to the time-dependent release of Oregon Green-modified dextran and (b) time-dependent release of tetramethylrhodamine modified dextran; panel II, treatment of the structure with strand (**12**) [(a) release of Oregon Green-modified dextran; (b) release of tetramethylrhodamine-modified dextran]; panel III, treatment of the hybrid structure with strands (**6**) and (**12**) [(a) release of Oregon Green-modified dextran; (b) release of tetramethylrhodamine-modified dextran].

EXPERIMENTAL SECTION

Materials. Tris(hydroxymethyl)aminomethane (Tris), potassium chloride, magnesium nitrate, ammonium persulfate (APS), N,N,N′,N′-Tetramethylethylenediamine (TEMED), acrylamide solution (40%), and 18-crown-6 ether were purchased from Sigma-Aldrich. SYBR Green I and Oregon Green Dextran (MW = 70 KD) were purchased from Life Technologies Corporation (USA). Gel Red and Gel Green were purchased from Biotium, Inc., USA. Ultrapure water purified by a NANOpure Diamond instrument (Barnstead International, Dubuque, IA, USA) was used to prepare all of the solutions.

The following nucleic acid sequences (Integrated DNA Technologies Inc., Coralville, IA) were used in the study: (1) 5′-acrydite-AAA TTC GCG CGA A-3′; (2) 5′-acrydite-AAG GGT TAG GG-3′; (3) 5′-acrydite-AAA CCC CTA ACC CC-3′; (4) 5′-acrydite-AAA TCC CTG CCA AG-3′; (5) 5′-acrydite-AAACTT GGC AGG GA A CGC AGAC-3′; (6) 5′-CAT GTC GGG TCTG CGT TCCCTGC-3′; (7) 5′-GG GAA CGC AGA CCC GAC ATG-3′; (8) 5′-acrydite-CCT TAT CAT ATC TCT AGA CTA TCA AC-3′; (9) 5′-acrydite-GTT GAT AGT CTA GAG ATA TGA TAA GG-3′; (10) 5′-acrydite-AAA TCA ACG CCG AG-3′; (11) 5′-acrydite-AAA CTC GGC GTT GA AAGG ATG-3′; (12) 5′-GCC ATT CTC ATC CTT TCA ACG CC-3′; (13) 5′-GTT GA AAGG ATG AGA ATG GC-3′.

Synthesis of the Acrylamide/Acrydite-Nucleic Acid Copolymers. The system shown in Figure 1A consisting of the duplex/G-quadruplex cross-linked hydrogel was prepared as follows: A buffer solution (Tris-HCl, 10 mM, pH = 8.0), 200 μL, that included 2% acrylamide and the acrydite-modified DNA strands (**1**), 0.24 mM, and (**2**), 1.44 mM, was prepared. Nitrogen was bubbled through the solution. Subsequently, 5 μL of a 0.5 mL aqueous solution that included 50 mg APS and 25 μL TEMED was added to each of the monomer solutions. The resulting solution was allowed to polymerize at room temperature for 5 min, and then, the solution was further polymerized at 4 °C for 12 h. The resulting copolymers were purified from unreacted monomer units, salts, and the initiator, using a Microcon (Millipore) spin filter unit (MWCO 10 kDa). The purified

DOI: 10.1021/jacs.5b06510
J. Am. Chem. Soc. 2015, 137, 15723−15731

polymer was removed from the filter and dried under a gentle nitrogen gas flow. The concentrations of the copolymer chains and the ratio of the acrylamide/acrydite-nucleic acid units were determined spectroscopically.

For other hydrogel systems, the procedures to prepare the polymer chains were similar, yet different acrydite-modified DNA strands were used to prepare the respective hydrogels.

For the system shown in Figure 2A, hydrogel A consisting of the duplex/i-motif cross-linked hydrogel: A buffer solution (Tris-HCl, 10 mM, pH = 8.0), 200 μL, that included 2% acrylamide and the acrydite-modified DNA strands (**1**), 0.24 mM, and (**3**), 1.28 mM, was used for the polymerization.

For the system shown in Figure 4A, consisting of domain A composed of two kinds of duplexes cross-linked hydrogel: A buffer solution (Tris-HCl, 10 mM, pH = 8.0), 200 μL, that included 2% acrylamide and the acrydite-modified DNA strands (**1**), 0.24 mM, (**4**), 0.27 mM, (**5**), 0.27 mM, and (**8**), 0.24 mM, was used for the polymerization.

For the system shown in Figure 4A, consisting of domain B composed of two kinds of duplexes cross-linked hydrogel: A buffer solution (Tris-HCl, 10 mM, pH = 8.0), 200 μL, that included 2% acrylamide and the acrydite-modified DNA strands (**1**), 0.24 mM, (**10**), 0.27 mM, (**11**), 0.27 mM, and (**9**), 0.24 mM, was used for the polymerization.

For the determination of the loading of the different nucleic acid tethers in the acrylamide copolymer chains, see Supporting Information.

Preparation of a Triangle-Shaped Hydrogel and the Trigger-Induced Transitions between Shaped Hydrogel and Shapeless States. To form a triangle-shaped duplex/G-quadruplex cross-linked hydrogel, the dried copolymer sample P_1 was dissolved in a 200 μL Tris-acetate buffer (100 mM Tris-Acetate, 100 mM $MgCl_2$, pH 5.0) to yield a mixture containing 1.32 mM nucleic acids. The resulting mixture was heated to 90 °C, to yield a homogeneous aqueous polymer solution. The hot solution was poured into a triangle-shaped tetrafluoroethylene mold, and allowed to cool down to room temperature. A K^+ ion solution (200 mM) was added to the viscous composite in the mold, allowing the formation of the hydrogel stabilized by the duplex/G-quadruplex. After incubation for 4 h, the resulting shaped duplex/G-quadruplex cross-linked hydrogel was removed from the mold.

To form a triangle-shaped duplex/i-motif cross-linked hydrogel, or the two duplex cross-linked hydrogel, the dried copolymer chains were dissolved in a 200 μL Tris-acetate buffer (100 mM Tris-Acetate, 100 mM $MgCl_2$, pH 5.0) to yield mixtures containing 1.28, 0.83, and 0.78 mM nucleic acids, respectively. The resulting mixture was heated to 90 °C, to yield a homogeneous aqueous polymer solution. The hot solution was poured into a triangle-shaped tetrafluoroethylene mold, and allowed to cool down to room temperature for 2 h.The resulting shaped hydrogel was removed from the mold, respectively.

For the transitions of the duplex/G-quadruplex cross-linked shaped hydrogel to a soft and shapeless state and its recovery to the shaped structure, the triangle-shaped structure was immersed in a Tris-acetate buffer, pH = 5.0, that included 18-crown-6 ether, 200 mM, and $MgCl_2$, 100 mM, for 2 h. The surrounding solution was removed to yield an amorphous, nonshaped phase of the polymer. To recover the shaped hydrogel, a Tris-acetate buffer, pH = 5.0, that included KCl, 200 mM, and $MgCl_2$, 100 mM, was added to the amorphous matrix, and the recovery of the polymer shaped structure occurred within 2 h. The surrounding solution was removed, and the shaped hydrogel kept its structure for several hours with no noticeable changes. It should be noted that the hydrogel was stained with Gel Red.

For the transitions of the duplex/i-motif cross-linked shaped hydrogel to a shapeless state and its recovery to the shaped structure, the triangle-shaped structure was immersed in a Tris-acetate buffer, pH = 8.0, that included $MgCl_2$, 100 mM, for 0.5 h. The surrounding solution was removed to yield an amorphous, nonshaped phase of the polymer. To recover the shaped hydrogel, a Tris-acetate buffer, pH = 5.0, that included $MgCl_2$, 100 mM, was added to the amorphous state, and the recovery of the polymer shaped structure occurred within 0.5 h. The surrounding solution was removed, and the shaped hydrogel kept its structure for several hours with no noticeable changes. It should be noted that the hydrogel was stained with SYBR Green I.

For the transitions of the two different duplexes cross-linked hydrogel ((**1**)/(**1**):(**4**)/(**5**) or (**1**)/(**1**):(**10**)/(**11**)) to a shapeless state and its recovery to the shaped structure, the triangle-shaped structure was immersed in a Tris-acetate buffer (with 30 μL, 5 mM (**6**) or (**12**)), pH = 5.0, that included $MgCl_2$, 100 mM, for 4 h. The surrounding solution was removed to yield an amorphous, nonshaped phase of the polymer. To recover the shaped hydrogel, a Tris-acetate buffer (with 30 μL, 5 mM (**7**) or (**13**)), pH = 5.0, that included $MgCl_2$, 100 mM, was added to the amorphous matrix, and the recovery of the polymer shaped structure occurred within 4 h. The surrounding solution was removed, and the shaped hydrogel kept its structure for several hours with no noticeable changes. It should be noted that the hydrogels were stained with SYBR Green I and Gel Red, respectively. Furthermore, we note that, in the strand-displacement stimulated transitions of the shaped hydrogel to the soft and shapeless state, and back to the shaped structure, we use an excess of the fuel (e.g., (**6**)) and antifuel (e.g., (**7**)) strands. These relatively high concentrations of the fuel/antifuel strands are used to enhance the strand displacement processes and the accompanying cyclic hydrogel-to-liquid transitions. Also, it should be noted that the antifuel strand, e.g., (**7**), selectively hybridizes with (**6**) to release the duplex (**6**)/(**7**) and allow the reannealing of (**4**) with (**5**) to form the duplex (**4**)/(**5**). Note, however, that although (**7**) includes a complementary domain to (**4**), the formation of the possible duplex (**4**)/(**7**) is disfavored since the duplex (**4**)/(**5**) is substantially more stable than (**4**)/(**7**) due to the higher number of complementary bases.

The formation of two- or three-arrowhead-shaped hydrogel followed the procedures described in the captions of Figure 2B, Figure 4B, and Figure 5B. The stimuli-triggered transitions of the two- or three-arrowhead-shaped hydrogels between shaped hydrogel structures and shapeless states were achieved by applying the conditions mentioned above for each hydrogel, respectively. It should be noted that, in the three-arrowhead-shaped hydrogel system, in order to bridge the duplex/i-motif cross-linked domain "C" to the system, this domain "C" was functionalized with the DNA strand, L_2 (**9**). The hybridization of L_1/L_2, (**8**)/(**9**), bridged domain A and domain C. In the three-arrowhead-shaped hydrogel system, duplex/i-motif cross-linked domain C was stained with Gel Green. It should be noted that the entire two-arrowhead or three-arrowhead hybrid structures shown in Figure 4 or Figure 5 were subjected to the respective triggers, and only the stimuli-responsive domains of the structures responded to these triggers.

The rheology experiments and SEM imaging experiments characterizing the different hydrogels and additional experimental details are provided in the Supporting Information.

■ ASSOCIATED CONTENT

Supporting Information

The Supporting Information is available free of charge on the ACS Publications website at DOI: 10.1021/jacs.5b06510.

Details of determination of the loading of the different nucleic acid tethers in the acrylamide copolymer chains, rheology experiments, and SEM imaging experiments (PDF)

■ AUTHOR INFORMATION

Corresponding Author

*willnea@vms.huji.ac.il

Author Contributions

C.H.-L. and W.G. contributed equally.

Notes

The authors declare no competing financial interest.

DOI: 10.1021/jacs.5b06510
J. Am. Chem. Soc. 2015, 137, 15723−15731

■ ACKNOWLEDGMENTS

This research is supported by the NanoSensoMach ERC Advanced Grant (#267574) under the European Union's Seventh Framework Programme (FP7/2007-2013).

■ REFERENCES

(1) (a) Lendlein, A.; Kelch, S. *Angew. Chem., Int. Ed.* **2002**, *41*, 2034. (b) Liu, C.; Qin, H.; Mather, P. T. *J. Mater. Chem.* **2007**, *17*, 1543. (c) Yoshida, M.; Langer, R.; Lendlein, A.; Lahann, J. *J. Macromol. Sci., Polym. Rev.* **2006**, *46*, 347. (d) Meng, H.; Li, G. *Polymer* **2013**, *54*, 2199. (e) Julich-Gruner, K. K.; Löwenberg, C.; Neffe, A. T.; Behl, M.; Lendlein, A. *Macromol. Chem. Phys.* **2013**, *214*, 527. (f) Mohr, R.; Kratz, K.; Weigel, T.; Lucka-Gabor, M.; Moneke, M.; Lendlein, A. *Proc. Natl. Acad. Sci. U. S. A.* **2006**, *103*, 3540.

(2) (a) Khaldi, A.; Elliott, J. A.; Smoukov, S. K. *J. Mater. Chem. C* **2014**, *2*, 8029. (b) Ge, Q.; Westbrook, K. K.; Mather, P. T.; Dunn, M. L.; Qi, H. J. *Smart Mater. Struct.* **2013**, *22*, 055009. (c) Paik, I. H.; Goo, N. S.; Jung, Y. C.; Cho, J. W. *Smart Mater. Struct.* **2006**, *15*, 1476.

(3) (a) Qiu, Y.; Park, K. *Adv. Drug Delivery Rev.* **2001**, *53*, 321. (b) Behl, M.; Zotzmann, J.; Lendlein, A. *Adv. Polym. Sci.* **2009**, *226*, 1.

(4) (a) Koerner, H.; Price, G.; Pearce, N. A.; Alexander, M.; Vaia, R. A. *Nat. Mater.* **2004**, *3*, 115. (b) Lendlein, A.; Langer, R. *Science* **2002**, *296*, 1673. (c) Kunzelman, J.; Chung, T.; Mather, P. T.; Weder, C. *J. Mater. Chem.* **2008**, *18*, 1082. (d) Ecker, M.; Pretsch, T. *RSC Adv.* **2014**, *4*, 286. (e) Ebara, M.; Uto, K.; Idota, N.; Hoffman, J. M.; Aoyagi, T. *Soft Matter* **2013**, *9*, 3074. (f) Pretsch, T.; Ecker, M.; Schildhauer, M.; Maskos, M. *J. Mater. Chem.* **2012**, *22*, 7757.

(5) Wang, F.; Lu, C. H.; Willner, I. *Chem. Rev.* **2014**, *114*, 2881.

(6) (a) Liu, D.; Balasubramanian, S. *Angew. Chem., Int. Ed.* **2003**, *42*, 5734. (b) Sharma, J.; Chhabra, R.; Yan, H.; Liu, Y. *Chem. Commun.* **2007**, 477. (c) Wang, W.; Yang, Y.; Cheng, E.; Zhao, M.; Meng, H.; Liu, D.; Zhou, D. *Chem. Commun.* **2009**, 824. (d) Wang, C.; Huang, Z.; Lin, Y.; Ren, J.; Qu, X. *Adv. Mater.* **2010**, *22*, 2792. (e) Elbaz, J.; Shimron, S.; Willner, I. *Chem. Commun.* **2010**, *46*, 1209. (f) Wang, X.; Huang, J.; Zhou, Y.; Yan, S.; Weng, X.; Wu, X.; Deng, M.; Zhou, X. *Angew. Chem., Int. Ed.* **2010**, *49*, 5305. (g) Shimron, S.; Magen, N.; Elbaz, J.; Willner, I. *Chem. Commun.* **2011**, *47*, 8787.

(7) (a) Monchaud, D.; Yang, P.; Lacroix, L.; Teulade-Fichou, M. P.; Mergny, J. L. *Angew. Chem., Int. Ed.* **2008**, *47*, 4858. (b) Ono, A.; Cao, S. Q.; Togashi, H.; Tashiro, M.; Fujimoto, T.; Machinami, T.; Oda; Miyake, S. Y.; Okamoto, I.; Tanaka, Y. *Chem. Commun.* **2008**, 4825. (c) Han, D.; Kim, Y. R.; Oh, J. W.; Kim, T. H.; Mahajan, R. K.; Kim, J. S.; Kim, H. *Analyst* **2009**, *134*, 1857. (d) Li, T.; Shi, L.; Wang, E.; Dong, S. *Chem. - Eur. J.* **2009**, *15*, 3347. (e) Shimron, S.; Elbaz, J.; Henning, A.; Willner, I. *Chem. Commun.* **2010**, *46*, 3250.

(8) (a) Liu, Y.; Sen, D. *J. Mol. Biol.* **2004**, *341*, 887. (b) Liang, X.; Nishioka, H.; Takenaka, N.; Asanuma, H. *ChemBioChem* **2008**, *9*, 702. (c) Kang, H.; Liu, H.; Phillips, J. A.; Cao, Z.; Kim, Y.; Chen, Y.; Yang, Z.; Li, J.; Tan, W. *Nano Lett.* **2009**, *9*, 2690. (d) Han, D.; Huang, J.; Zhu, Z.; Yuan, Q.; You, M.; Chen, Y.; Tan, W. *Chem. Commun.* **2011**, *47*, 4670. (e) Yang, Y.; Endo, M.; Hidaka, K.; Sugiyama, H. *J. Am. Chem. Soc.* **2012**, *134*, 20645. (f) You, M.; Huang, F.; Chen, Z.; Wang, R. W.; Tan, W. *ACS Nano* **2012**, *6*, 7935. (g) Zou, Y.; Chen, J.; Zhu, Z.; Lu, L.; Huang, Y.; Song, Y.; Zhang, H.; Kang, H.; Yang, C. J. *Chem. Commun.* **2013**, *49*, 8716.

(9) (a) Liu, D.; Bruckbauer, A.; Abell, C.; Balasubramanian, S.; Kang, D. J.; Klenerman, D.; Zhou, D. *J. Am. Chem. Soc.* **2006**, *128*, 2067. (b) Liedl, T.; Olapinski, M.; Simmel, F. C. *Angew. Chem., Int. Ed.* **2006**, *45*, 5007. (c) Meng, H.; Yang, Y.; Chen, Y.; Zhou, Y.; Liu, Y.; Chen, X.; Ma, H.; Tang, Z.; Liu, D.; Jiang, L. *Chem. Commun.* **2009**, 2293. (d) Wang, Z. G.; Elbaz, J.; Willner, I. *Nano Lett.* **2011**, *11*, 304. (e) Gao, X. Y.; Li, X. H.; Xiong, W. M.; Huang, H. M.; Lin, Z. Y.; Qiu, B.; Chen, G. N. *Electrochem. Commun.* **2012**, *24*, 9. (f) Qi, X. J.; Lu, C. H.; Liu, X.; Shimron, S.; Yang, H. H.; Willner, I. *Nano Lett.* **2013**, *13*, 4920.

(10) (a) Li, J.; Tan, W. *Nano Lett.* **2002**, *2*, 315. (b) Niemeyer, C. M.; Adler, M. *Angew. Chem., Int. Ed.* **2002**, *41*, 3779. (c) Uno, S.-N.; Dohno, C.; Bittermann, H.; Malinovskii, V. L.; Häner, R.; Nakatani, K. *Angew. Chem., Int. Ed.* **2009**, *48*, 7362.

(11) (a) Li, T.; Dong, S.; Wang, E. *J. Am. Chem. Soc.* **2010**, *132*, 13156. (b) Sannohe, Y.; Endo, M.; Katsuda, Y.; Hidaka, K.; Sugiyama, H. *J. Am. Chem. Soc.* **2010**, *132*, 16311. (c) Ge, B.; Huang, Y. C.; Sen, D.; Yu, H. Z. *Angew. Chem., Int. Ed.* **2010**, *49*, 9965. (d) Liu, X.; Niazov-Elkan, A.; Wang, F.; Willner, I. *Nano Lett.* **2013**, *13*, 219.

(12) (a) Yurke, B.; Turberfield, A. J.; Mills, A. P., Jr.; Simmel, F. C.; Neumann, J. L. *Nature* **2000**, *406*, 605. (b) Yan, H.; Zhang, X.; Shen, Z.; Seeman, N. C. *Nature* **2002**, *415*, 62. (c) Simmel, F. C.; Dittmer, W. U. *Small* **2005**, *1*, 284. (d) Wang, F.; Liu, X.; Willner, I. *Angew. Chem., Int. Ed.* **2015**, *54*, 1098. (e) Beissenhirtz, M. K.; Willner, I. *Org. Biomol. Chem.* **2006**, *4*, 3392. (f) Bath, J.; Turberfield, A. J. *Nat. Nanotechnol.* **2007**, *2*, 275. (g) Teller, C.; Willner, I. *Curr. Opin. Biotechnol.* **2010**, *21*, 376. (h) Krishnan, Y.; Simmel, F. C. *Angew. Chem., Int. Ed.* **2011**, *50*, 3124.

(13) (a) Roh, Y. H.; Ruiz, R. C. H.; Peng, S.; Lee, J. B.; Luo, D. *Chem. Soc. Rev.* **2011**, *40*, 5730. (b) Liu, J. *Soft Matter* **2011**, *7*, 6757. (c) Xiong, X.; Wu, C.; Zhou, C.; Zhu, G.; Chen, Z.; Tan, W. *Macromol. Rapid Commun.* **2013**, *34*, 1271. (d) Peng, S.; Derrien, T. L.; Cui, J.; Xu, C.; Luo, D. *Mater. Today* **2012**, *15*, 5.

(14) Um, S. H.; Lee, J. B.; Park, N.; Kwon, S. Y.; Umbach, C. C.; Luo, D. *Nat. Mater.* **2006**, *5*, 797.

(15) (a) Wei, B.; Cheng, I.; Luo, K. Q.; Mi, Y. *Angew. Chem.* **2008**, *120*, 337. (b) Yang, H. H.; Liu, H.; Kang, H.; Tan, W. *J. Am. Chem. Soc.* **2008**, *130*, 6320. (c) Zhu, Z.; Wu, C.; Liu, H.; Zou, Y.; Zhang, X.; Kang, H.; Yang, C. J.; Tan, W. *Angew. Chem., Int. Ed.* **2010**, *49*, 1052. (d) Yan, L.; Zhu, Z.; Zou, Y.; Huang, Y.; Liu, D.; Jia, S.; Xu, D.; Wu, M.; Zhou, Y.; Zhou, S.; Yang, C. J. *J. Am. Chem. Soc.* **2013**, *135*, 3748.

(16) (a) Liedl, T.; Dietz, H.; Yurke, B.; Simmel, F. C. *Small* **2007**, *3*, 1688. (b) Lu, C. H.; Qi, X. J.; Orbach, R.; Yang, H. H.; Mironi-Harpaz, I.; Seliktar, D.; Willner, I. *Nano Lett.* **2013**, *13*, 1298. (c) Guo, W.; Qi, X. J.; Orbach, R.; Lu, C. H.; Freage, L.; Mironi-Harpaz, I.; Seliktar, D.; Yang, H. H.; Willner, I. *Chem. Commun.* **2014**, *50*, 4065. (d) Xing, Y.; Cheng, E.; Yang, Y.; Chen, P.; Zhang, T.; Sun, Y.; Yang, Z.; Liu, D. *Adv. Mater.* **2011**, *23*, 1117. (e) Lin, H.; Zou, Y.; Huang, Y.; Chen, J.; Zhang, W. Y.; Zhuang, Z.; Jenkins, G.; Yang, C. J. *Chem. Commun.* **2011**, *47*, 9312. (f) Guo, W.; Lu, C. H.; Qi, X. J.; Orbach, R.; Fadeev, M.; Yang, H. H.; Willner, I. *Angew. Chem., Int. Ed.* **2014**, *53*, 10134. (g) Cheng, E.; Xing, Y.; Chen, P.; Yang, Y.; Sun, Y.; Zhou, D.; Xu, L.; Fan, Q.; Liu, D. *Angew. Chem., Int. Ed.* **2009**, *48*, 7660.

(17) Ren, J.; Hu, Y.; Lu, C. H.; Guo, W.; Aleman-Garcia, M. A.; Ricci, F.; Willner, I. *Chem. Sci.* **2015**, *6*, 4190.

(18) Soontornworajit, B.; Zhou, J.; Zhang, Z.; Wang, Y. *Biomacromolecules* **2010**, *11*, 2724.

(19) Joseph, K. A.; Dave, N.; Liu, J. *ACS Appl. Mater. Interfaces* **2011**, *3*, 733.

(20) He, X.; Wei, B.; Mi, Y. *Chem. Commun.* **2010**, *46*, 6308.

(21) Lilienthal, S.; Shpilt, Z.; Wang, F.; Orbach, R.; Willner, I. *ACS Appl. Mater. Interfaces* **2015**, *7*, 8923.

(22) Lee, J. B.; Peng, S.; Yang, D.; Roh, Y. H.; Funabashi, H.; Park, N.; Rice, E. J.; Chen, L.; Long, R.; Wu, M.; Luo, D. *Nat. Nanotechnol.* **2012**, *7*, 816.

(23) Guo, W.; Lu, C. H.; Orbach, R.; Wang, F.; Qi, X.-J.; Cecconello, A.; Seliktar, D.; Willner, I. *Adv. Mater.* **2015**, *27*, 73.

DOI: 10.1021/jacs.5b06510
J. Am. Chem. Soc. 2015, 137, 15723−15731